Temporal and spacial evolution of bursts in creep rupture

Zsuzsa Danku and Ferenc Kun*
Department of Theoretical Physics, University of Debrecen, P.O. Box 5, H-4010 Debrecen, Hungary

We investigate the temporal and spacial evolution of single bursts emerging in heterogeneous materials under a constant external load. Based on a fiber bundle model we demonstrate that when the load redistribution is localized along a propagating crack front, the average temporal shape of pulses has a right handed asymmetry due to the gradual acceleration of bursts. For long range interaction, however, a symmetric shape with parabolic functional form is obtained. In spite of the compact internal structure, the external frontier of bursts proved to be a fractal with dimension $D_f = 1.25$. We show that the geometry of avalanches in systems dominated by short range interactions exhibits an astonishing robustness falling in the universality class of Loop Erased Random Walks. Our analysis revealed that the pulse shape and spatial evolution of bursts are correlated which can be exploited in materials' testing.

PACS numbers: 89.75.Da, 46.50.+a, 05.90.+m

Crackling noise is a generic feature of a wide variety of slowly driven dynamic systems such as ferromagnetic materials, plastically deforming crystals, superconductors, fracture processes of heterogeneous materials and earthquakes [1–5]. Measuring crackling noise is the primary source of information about the microscopic dynamics of these systems having an enormous technological importance for the development of non-destructive materials' testing methods [5]. Analyzing the time series of crackling events as a stochastic point process, it was shown that crackling phenomena exhibit a high degree of universality [1, 4]: the size (energy) and duration of events, furthermore, the waiting times in between are characterized by power law distributions with the same exponents in systems of different microscopic dynamics. As a major advancement of the field, recently it has been demonstrated for Barkhausen noise that there are unique features of crackling which go beyond universality, i.e. the average temporal shape of single burst pulses proved to provide direct information about the presence and nature of correlations in the microscopic dynamics [2, 3, 6–8].

Here we present a theoretical investigation of crackling noise emerging during the creep rupture of heterogeneous materials focusing on single burst dynamics. Creep rupture has a high technological importance for the safety of construction components and it is at the core of natural catastrophes such as landslides, stone and snow avalanches, as well [9]. Crackling during creep is the consequence of the intermittent nucleation and propagation of cracks which generate acoustic bursts. In spite of the intensive experimental and theoretical research on rupture phenomena [9–17], the temporal and spatial evolution of single bursts and their relevance for applications still remained an open fundamental problem. Based on a fiber bundle model of heterogeneous materials a rich spectrum of novel aspects are revealed having also technological importance: we demonstrate that the average temporal shape of burst pulses encodes information about the range of load redistribution following failure events. The geometry of bursts proved to have an astonishing robustness falling in the universality class of Loop Erased Random Walks when short range interaction dominates the load redistribution. Our investigation verifies that for single bursts the temporal pulse shape and the spatial form relative to the crack front are correlated, which can be exploited for materials testing methods.

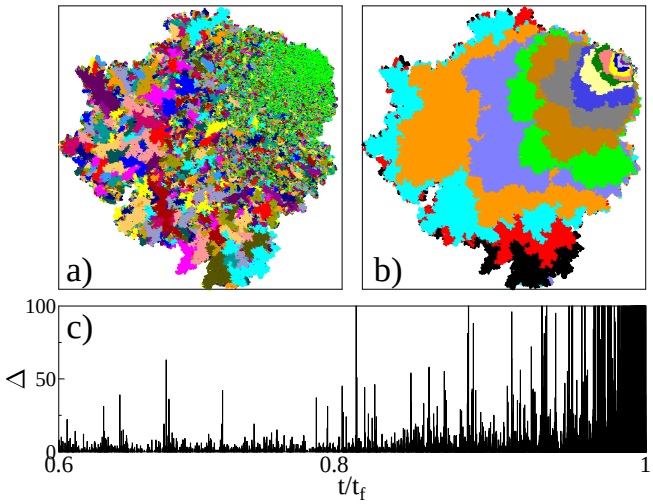

FIG. 1. (Color online) (a) Bursting activity during the creep rupture of a fiber bundle of size $L = 401$. Slowly damaging fibers (green) trigger bursts of immediate breaking (randomly selected colors different from green). The crack started in the upper right corner of the figure. (b) Advancement of the front of the same crack obtained such that fibers broken in a time interval have the same color. (c) Time series of bursts of (a) as a stochastic point process.

To investigate the creep rupture of heterogeneous materials we use a generic fiber bundle model (FBM) introduced recently [18–20]: the sample is discretized in terms of a bundle of parallel fibers organized on a square lattice of side length $L = 401$ having a brittle response with

identical Young modulus E. The bundle is subject to a constant external load σ_0 below the fracture strength σ_c of the system parallel to the direction of fibers. It is a crucial element of the model that fibers break due to two physical mechanisms: immediate breaking occurs when the local load σ_i on fibers exceeds their fracture strength σ_{th}^i, $i = 1, \ldots, N = L^2$. Time dependence is introduced in such a way that those fibers, which remained intact, undergo an aging process accumulating damage $c_i(t)$. The damage mechanism represents the environmentally induced slowly developing aging of materials such as corrosion cracking and thermally activated degradation [18–20]. The rate of damage accumulation Δc_i is assumed to have a power law dependence on the local load $\Delta c_i = a\sigma_i^\gamma \Delta t$, where a is a constant and the exponent γ controls the time scale of the aging process with $0 \leq \gamma < +\infty$. Fibers can tolerate only a finite amount of damage so that when $c_i(t)$ exceeds the local damage threshold c_i^{th} the fiber breaks. Each breaking event is followed by a redistribution of load over the remaining intact fibers. In order to capture the effect of stress concentration around cracks, we assume localized load sharing, i.e. after failure events the load of broken fibers is equally redistributed over their intact nearest neighbors on the lattice.

It has to be emphasized that in our damage induced creep model there are two sources of disorder, namely, the structural disorder of the material which is represented by the randomness of breaking thresholds σ_i^{th}, c_i^{th}, $i = 1, \ldots, N$, and the heterogeneous stress field generated by the short ranged load redistribution. For simplicity, we assume that both thresholds are uniformly distributed in the interval $[1-\delta, 1+\delta]$, where $\delta = 1$ for σ^{th}. To promote the effect of stress concentrations low damage disorder is considered $\delta = 0.2$ while the exponent γ of the damage accumulation law is set to a high value $\gamma = 5$ (the constant a is fixed to 1). This parameter setting ensures that a single growing crack emerges where all failures get localized along the propagating crack front [20]. Our model has proven very successful in reproducing measured creep behavior and statistics of crackling burst time series for various types of materials [18–20].

Figure 1(a) presents a representative example of the time evolution of a crack in the fiber bundle under the load $\sigma_0/\sigma_c = 0.01$. The separation of time scales of the slow damage process and of immediate breaking leads to a highly complex time evolution in agreement with experiments [18, 19]: after the crack nucleated, at early times fibers mostly break due to slow damaging. Since damage breakings are localized, an advancing crack front emerges along which all the stress of broken fibers is concentrated. Beyond a certain crack size the subsequent load increments at the crack front become sufficient to trigger bursts of immediate breakings locally accelerating the front. As a consequence, the time evolution of creep rupture occurs as a series of bursts corresponding

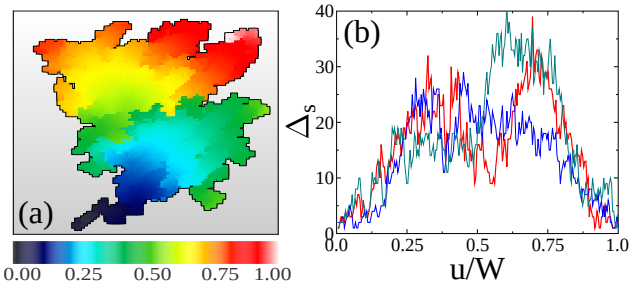

FIG. 2. (Color online) (a) Temporal and spatial evolution of a single burst of size $\Delta = 3485$. The color code represents the normalized time $0 \leq u/W \leq 1$. The burst starts from a small spot of broken fibers (*blue*) at the bottom left corner, then it gradually expands (*green, yellow, red*) and finally stops again in a small spot (*white*) at the top right corner. (b) The size of sub-bursts Δ_s as a function of u/W. The red curve corresponds to the burst of (a). Two additional examples are presented with the same duration $W = 253$.

to the nucleation and propagation of cracks, separated by silent periods of slow damaging. The size of bursts Δ is defined as the number of fibers breaking in a correlated trail which was triggered by a slow sequence of damage events. For clarity, in Fig. 1(b) the crack front is presented at several times during the evolution of the system. The bursts of Fig. 1(a) are intermittent local steps of the advancing front, which can be recorded by acoustic emission techniques. In Fig. 1(c) we also present the time series of bursts, i.e. the burst size Δ is plotted as a function of time t where it occurred normalized with the lifetime t_f of the system [11–14, 19, 20].

Bursts typically start with the immediate breaking of a few fibers neighboring the last damaging event along the propagating crack front. As a consequence of subsequent load redistributions, additional breakings are triggered so that burst gradually evolve through sub-avalanches and stop when all the intact fibers along the burst boundary can sustain the elevated load. It can be observed in Fig. 2 for a burst of size $\Delta = 3485$ that the outbreak starts from a small localized spot which then gradually expands to a broad region as sub-bursts grow followed by the subsequent reduction of the breaking activity. The temporal profile of bursts can be characterized by recording the number of fibers Δ_s breaking in sub-avalanches as a function of the internal time step u over the entire duration W of the burst, where $1 \leq u \leq W$ holds. Comparing $\Delta_s(u)$ curves of bursts of the same duration $W = 253$ in Fig. 2(b) a rather irregular behavior can be pointed out due to the stochastic nature of avalanche dynamics. It follows from the above arguments that the temporal evolution of breaking avalanches $\Delta_s(u)$ is responsible for the complex pulse shape of acoustic and electromagnetic signals in crackling noise measurements [10–14].

For the quantitative characterization we determined

the average pulse shape $\langle \Delta_s(u,W) \rangle$ which is presented in Fig. 3(a) as a function of time u varying the pulse duration W in a broad range. It is important to note that the $\langle \Delta_s(u,W) \rangle$ curves have a right-handed asymmetry, i.e. they can be described by a nearly parabolic shape where the maximum of the inverted parabola is shifted from the middle ($W/2$) to higher values. Increasing the avalanche duration the maximum of the curves get higher, however, the functional form remains the same. Figure 3(b) demonstrates that rescaling $\langle \Delta_s(u,W) \rangle$ with an appropriate power α of the duration W, the pulse shapes of different durations W can be collapsed on a master curve as a function of the normalized time $x = u/W$. The good quality data collapse implies the scaling form

$$\langle \Delta_s(u,W) \rangle = W^{\alpha} f(u/W), \tag{1}$$

where both the scaling function $f(x)$ and the scaling exponent α encodes important information about the jerky crack propagation during the process of creep rupture. The right-handed asymmetry of the scaling function $f(x)$ shows that bursts start slowly and gradually accelerate due to the subsequent load redistribution and finally the burst stops suddenly as the front gets pinned by a locally strong region. Careful data analysis has revealed that the average pulse shape of our model can be described by the functional form

$$f(x) = Ax(1-x)^{\beta}, \tag{2}$$

where the multiplication factor A determines the initial acceleration of bursts. The exponent β controls the degree of asymmetry of the pulse shape such that $\beta = 1$ yields a symmetric inverted parabola, while $\beta < 1$ describes the observed right-handed asymmetry. In Fig. 3(b) collapse was achieved with $\alpha = 0.7$, while the fit of the scaling function was obtained with the parameter values $A = 4.65$ and $\beta = 0.65$.

It follows from Eq. (1) that the average size of bursts $\langle \Delta \rangle = \int_0^W \langle \Delta_s(u) \rangle \, du$ [2] must scale with the burst duration as

$$\langle \Delta \rangle \sim W^{1+\alpha}. \tag{3}$$

To verify the above scaling structure we determined the function $\langle \Delta \rangle (W)$ numerically by directly averaging the size of bursts Δ at fixed durations W. It can be observed in Fig. 3(c) that the simulation results agree very well with the analytic prediction, however, the average burst size has a crossover at a threshold duration W_c between two power law regimes of different exponents. In the regime $W < W_c$ the average burst size proved to be proportional to the duration $\langle \Delta \rangle \sim W$ with $\alpha = 0$, which implies that small-sized avalanches behave like "creep lines" breaking a single fiber along the crack front in each subavalanche. Such line-shaped bursts have recently been found by the experiments of Ref. [15–17] during the propagation of a crack front in a heterogeneous material. Our

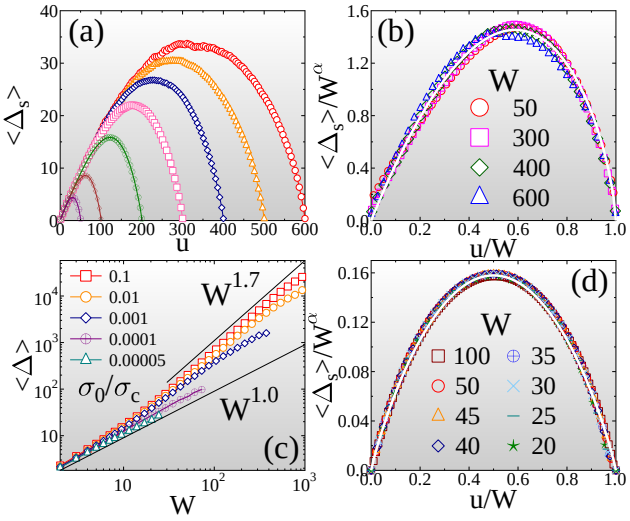

FIG. 3. (Color online) (a) Average pulse shapes for durations $W = 50, 100, 200, 300, 400, 500, 600$ from left to right for LLS FBMs obtained at the load $\sigma_0/\sigma_c = 0.01$. (b) Scaling collapse of average pulse shapes of different duration. (c) Average burst size $\langle \Delta \rangle$ as a function of duration W for several load values σ_0/σ_c. A crossover can be observed between two power law regimes of different exponents. (d) Scaling collapse of average pulse shapes of bursts in the mean field limit obtained with $\alpha = 1$. The white continuous lines in (b) and (d) represent fits with the scaling function Eq. (2).

results show that their pulse shape is not parabolic but instead they must have a flat, symmetric functional form. Large bursts $W > W_c$ are characterized by a higher scaling exponent α, which increases from 0 to 1 with increasing external load σ_0/σ_c. At higher load avalanche triggering becomes more efficient, hence, in Fig. 3(c) the size of creep lines, and hence, the crossover duration W_c are decreasing functions of σ_0/σ_c .

To quantify the degree of asymmetry of pulse shapes we calculated the skewness S as a function of W

$$S(W) = \frac{\frac{1}{W}\int_0^W du(u-\overline{u})^3 \langle \Delta_s(u,W) \rangle}{\frac{1}{W}\left[\int_0^W du(u-\overline{u})^2 \langle \Delta_s(u,W) \rangle\right]^{3/2}}, \tag{4}$$

where $\overline{u} = (1/W)\int_0^W \langle \Delta_s(u,W) \rangle \, u du$ denotes the mean of u [2]. Figure 4(a) demonstrates that the skewness S of our bursts is negative in agreement with the observed right handed asymmetry of pulse shapes, however, the value of S has a strong dependence on the pulse duration W: short pulses are flat and symmetric, hence, $S \approx 0$ follows in this range in agreement with the above scaling analysis of $\langle \Delta \rangle$. Bursts of high duration tend again to be symmetric, since as they evolve the structural disorder of the heterogeneous material becomes dominating, which favors symmetric pulse shapes [2–4, 6]. The most remarkable feature of the results is that at each load a characteristic time scale W_{max} emerges where the degree of asymmetry has a maximum. It can be observed

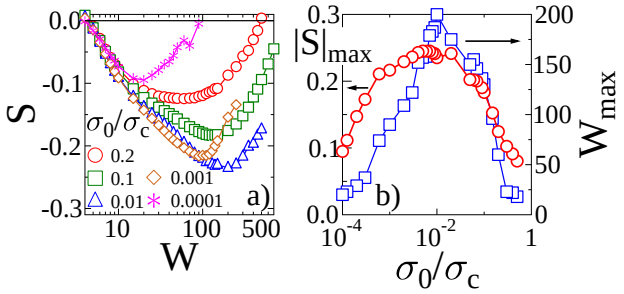

FIG. 4. (Color online) (a) Skewness S of temporal pulse shapes as a function of the duration W of bursts at different load values. The highest asymmetry characterized by the maximum $|S|_{max}$ of the absolute value of S is reached at load dependent durations W_{max}. (b) $|S|_{max}$ and W_{max} as function of the external load σ_0/σ_c.

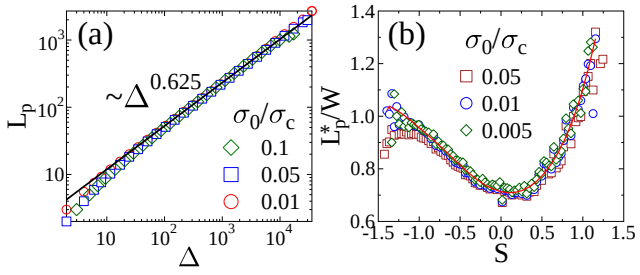

FIG. 5. (Color online) (a) Frontier length L_p as a function of burst size Δ. (b) The number of perimeter sites of bursts touching the crack front L_p^* divided by the burst duration W as a function of the corresponding skewness of the burst.

in Fig. 4(b) that both the characteristic duration W_{max} and strength of asymmetry $|S|_{max}$ of pulses have a strong dependence on the external load σ_0/σ_c, and they reach a maximum nearly at the same load $\sigma_0/\sigma_c \approx 0.01$. Note that the changing skewness implies that the parameters A and β of the scaling function $f(x)$ in Eq. (2) depend on the pulse duration W spanning the intervals $3 \leq A \leq 4.9$ and $0.6 \leq \beta \leq 1$. This also explains why the data collapse in Fig. 3(b) is not completely perfect.

In order to understand the role of the range of load sharing in shaping temporal pulses, we analyzed the mean field limit of our fiber bundle model [18–20]. In this limiting case the load of broken fibers is equally shared by all the remaining intact ones so that no stress concentration, and hence, no spatial correlation can arise in the bundle [21]. Based on the analogy of the evolution of mean field bursts to random walks, one can show analytically that the pulse shape is a symmetric inverted parabola [2–4, 6]. Fig. 3(d) presents the data collapse analysis of average pulse shapes of mean field simulations of a bundle of $N = 10^7$ fibers, where the symmetric parabolic shape of the scaling function $f(x)$ is evidenced. The high quality data collapse was obtained with the scaling exponent $\alpha = 1$. Other type of mean field models of avalanches provided similar results for slip events in plastically deforming solids and for avalanches of particle rearrangements in sheared granular matter [4]. For Barkhausen noise in thin films experimental and theoretical investigations revealed that due to the long-range nature of dipolar interactions the average shape of Barkhausen pulses is a symmetric inverted parabola [2]. Increasing the thickness of the ferromagnetic layer, Barkhausen signals develop a left-handed asymmetry due to the negative effective mass of domain walls generated by eddy currents [1, 3]. For our rupture process the gradual accumulation of load at the avalanche frontier introduces correlations of consecutive sub-avalanches which is then reflected by the temporal shape of pulses.

It can be observed in Fig. 1(a) and Fig. 2(a) that from geometrical point of view single bursts are compact objects, i.e. they do not contain islands of intact fibers. We calculated the radius of gyration R_g of bursts in terms of which the burst size Δ proved to have a power law functional form $\Delta \sim R_g^D$ with the exponent $D = 2$. The most remarkable feature of avalanches is that they have a complex frontier which reflects their growth dynamics (see Fig. 2). For the quantitative characterization we determined the number of perimeter sites L_p on the lattice as a function of the size of bursts Δ. In Fig. 5(c) a high quality power law is evidenced

$$L_p \sim \Delta^{\xi}, \tag{5}$$

where the exponent ξ was obtained as $\xi = 0.625 \pm 0.015$. This feature implies that the avalanche frontier is a fractal with fractal dimension $D_f = \xi D = 1.25 \pm 0.03$. It is important to emphasize that the fractal dimension D_f proved to be universal, i.e. it neither depends on the external load σ_0 nor on any details of damage accumulation such as γ, until single crack propagation is ensured in a heterogeneous environment. It is interesting to note that avalanches of other type of systems with short range interaction show a striking similarity to the bursts of our LLS FBM. The Abelian Sandpile Model (ASM) is a paradigmatic model of self organized criticality [22, 23] where topling (overstressed) lattice sites relax by redistributing sand grains over their local neighborhood. Majumdar showed that the frontiers of avalanches driven by short range redistribution in ASM can exactly be mapped to Loop Erased Random Walks (LERW) in two dimensions, and determined their fractal dimension exactly $D_f = 5/4$ [22]. Based on the growth dynamics, geometrical features, and robustness of the fractal dimension of burst perimeters we conjecture that breaking avalanches of FBMs fall in the universality class of LERWs similarly to avalanches of granular piles [22].

After starting from a localized spot, the avalanche spreads out, and hence, the overload which initiated it, gets redistributed in the surroundings. This expansion decreases the stress concentration along the evolving front so that it may get pinned and the avalanche stops.

Since a large amount of load has accumulated along the crack front, an avalanche has more chance to advance if sub-bursts involve fibers along the crack front, as well, instead of just propagating forward ahead of the crack front (see Fig. 1(a, b)). It has the very interesting consequence that the pulse shape of temporal evolution and of the geometry of avalanches with respect to the local position of the crack front get correlated. In order to quantify this correlation we measured the number of those perimeter sites L_p^* of bursts which are located at the crack front itself. In Fig. 5(d) the value of the ratio L_p^*/W is plotted as a function of the skewness S of the corresponding pulse. It can be observed that for symmetric pulses ($S \approx 0$) the ratio L_p^*/W has a low value which shows that these bursts were mainly moving forward ahead of the crack front where structural disorder dominates. However, for asymmetric pulses L_p^*/W increases which implies that the avalanche involves a large fraction of overloaded fibers which accelerates spreading along the crack front. Our result has the important consequence that by measuring pulse shapes of crackling noise one can infer the spatial propagation of bursts.

In conclusion, investigating the temporal and spatial dynamics of single bursts in a fiber bundle model we revealed a rich spectrum of novel aspects of rupture processes. The average temporal shape of burst pulses proved to be sensitive to the range of load redistribution in the system varying from symmetric parabolic shapes for long range to strongly asymmetric ones for short range interactions. Although, most real materials lie between the two limiting cases of load transfer, in highly disorder materials such as fiber reinforced composites, both equal and localized load sharing have direct relevance. For localized interaction we pointed out the emergence of a load dependent characteristic time scale of avalanche durations with the highest asymmetry. Since the evolution of bursts is controlled by the overloads at the avalanche frontier, we revealed that from the temporal pulse shape one can infer the spatial advancement of bursts with respect to the crack front. The growth dynamics of bursts leads to a compact spatial form, however, with a fractal frontier, which falls in the universality class of Loop Erased Random Walks similar to other short range avalanche processes. Besides its scientific importance, our work demonstrates the large potential of single burst analysis for the development of non-destructive materials' testing methods.

The work is supported by the projects TAMOP-4.2.2.A-11/1/KONV-2012-0036 and TAMOP-4.2.2/B-10/1-2010-0024. We acknowledge the support of OTKA K84157. This work was supported by the European Commissions by the Complexity-NET pilot project LOCAT.

* ferenc.kun@science.unideb.hu

[1] J. P. Sethna, K. A. Dahmen, and C. R. Meyers, Nature **410**, 242 (2001).
[2] S. Papanikolaou, et al., Nature Physics **7**, 316 (2011).
[3] S. Zapperi, C. Castellano, F. Colaiori, and G. Durin, Nature Physics **1**, 46 (2005).
[4] K. A. Dahmen, Y. Ben-Zion, and J. T. Uhl, Nature Physics **7**, 554 (2011).
[5] M. J. Alava, P. K. V. V. Nukala, and S. Zapperi, Adv Phys **55**, 349 (2006).
[6] A. Baldassarri, F. Colaiori, and C. Castellano, Phys. Rev. Lett. **90**, 060601 (2003).
[7] A. P. Mehta, A. C. Mills, K. A. Dahmen, and J. P. Sethna, Phys. Rev. E **65**, 046139 (2002).
[8] L. Laurson and M. J. Alava, Phys. Rev. E **74**, 066106 (2006).
[9] G. Niccolini, A. Carpinteri, A. Lacidogna, and A. Manuello, Phys. Rev. Lett. **106**, 108503 (2011).
[10] C. Maes, A. Van Moffaert, H. Frederix, and H. Strauven, Phys. Rev. B **57** 4987 (1998).
[11] H. Nechad, A. Helmstetter, R. El Guerjouma, and D. Sornette, Phys. Rev. Lett. **94**, 045501 (2005).
[12] J. Rosti, X. Illa, J. Koivisto, and M. J. Alava, J. Phys. D: Appl. Phys. **42**, 214013 (2009).
[13] S. Deschanel, L. Vanel, N. Godin, G. Vigier, and S. Ciliberto, J. Stat. Mech. P01018 (2009).
[14] A. Petri, G. Paparo, A. Vespignani, A. Alippi, and M. Costantini, Phys. Rev. Lett. **73**, 3423 (1994).
[15] K. J. Maloy, S. Santucci, J. Schmittbuhl, and R. Toussaint, Phys. Rev. Lett. **96**, 045501 (2006).
[16] D. Bonamy, S. Santucci, and L. Ponson, Phys. Rev. Lett. **101**, 045501 (2008).
[17] K. T. Tallakstad, R. Toussaint, S. Santucci, J. Schmittbuhl, and K. J. Maloy, Phys. Rev. E **83**, 046108 (2011).
[18] F. Kun, et al., J. Stat. Mech. **2007**, P02003 (2007).
[19] F. Kun, H. A. Carmona, J. S. Andrade Jr, and H. J. Herrmann, Phys. Rev. Lett. **100** 094301 (2008).
[20] Z. Halász, Zs. Danku, and F. Kun, Phys. Rev. E **85**, 016116 (2012).
[21] S. Pradhan, A. Hansen, and P. C. Hemmer, Phys. Rev. Lett. **95**, 125501 (2005); S. Pradhan, A. Hansen, and B. K. Chakrabarti, Rev. Mod. Phys. **82**, 499 (2010).
[22] S. N. Majumdar, Phys. Rev. Lett. **68**, 2329 (1992).
[23] D. Dhar, Phys. Rev. Lett. **64**, 1613 (1990).